High-Performance Control of Permanent Magnet Synchronous Motor using a Finite-Time Sliding Mode Observer and Super-Twisting Algorithm

Jing Nie [12], Yong Li [1] *, Gang Li [2]

[1] Automotive Engineering Research Institute, Jiangsu University, Zhenjiang, Chian
[2] School of Mechanical and Electrical Engineering, Chuzhou University, Chuzhou, China

Abstract. To enhance the tracking performance of the permanent magnet synchronous motor (PMSM) drive system in the face of changing operating conditions, such as variations in internal parameters and external load disturbances, this study proposed a new composite control strategy that combines the super-twisting sliding mode controller (STSM) with the finite-time sliding mode observer (FTSMO). The proposed methodology synergistically integrates the enhanced tracking precision and robust disturbance rejection properties inherent to the Second-order Tracking-Sliding Mode (STSM) controller with an innovative Finite-Time Sliding Mode Observer (FTSMO), thereby achieving significant improvements in system state estimation accuracy. The stability of the closed-loop PMSM drive system under the STSM+FTSMO framework is thoroughly analyzed and established using Lyapunov theory. The proposed composite control strategy's effectiveness is confirmed through both simulations and experimental outcomes. These findings illustrate that the proposed approach significantly surpasses conventional control methods, especially in managing external disturbances within the PMSM system. Significant enhancements are evident in start-up response, robustness against load variations, convergence speed, and steady-state performance.

Key words: permanent magnet synchronous motor (PMSM); super-twisting sliding mode controller (STSM); finite time sliding mode observer (FTSMO); perturbation resistance

1. INTRODUCTION

PMSM drives are already used in many industrial applications and possess high power density, excellent efficiency, and great reliability. The control of closed loop of PMSM drives is executed through the FOC strategy. The linear PI control strategy has been conventional to use in the design of speed controllers for PMSM drives due to its simplicity in implementation and ease of engineering application [1, 2, 3].

When applying permanent magnet synchronous motor systems in practical applications, there are inevitable uncertainties such as internal parameter variations and external load disturbances. Conventional controllers are not very efficient in the fast rejection of these disturbances, which worsen the system robustness and dynamic response. To overcome these limitations and enhance the control performance of the PMSM drive systems in uncertain and disturbance environments, many advanced control strategies have been proposed including adaptive control [4, 5], finite time control [6], predictive control [7, 8, 9], robust control [10, 11] and sliding mode control (SMC) [12, 13]. Among those methods, SMC has been recognized as one of the most efficient control strategies for the PMSM drive systems because of its high performance in tracking, robustness against parameter variations and sensitivity to load changes [14, 15]. However, the robustness of sliding mode controllers is usually fulfilled by large switching gains to cover the upper bound of the uncertainties. This makes SMC vulnerable to the so called chattering effect which is undesirable as it leads to control inaccuracy and actuator wear[16]. To this end, the super twisting sliding mode (STSM) control strategy has been proposed to solve this problem. This method actually smoothes the control force by incorporating the switching term into the integration scheme to avoid the chattering effect without compromising the accuracy of tracking and disturbance rejection. Hence, STSM has gained much attention and is used extensively in many areas [17]. However, the efficiency of the STSM control strategy is function of the knowledge of system disturbances and their compensation. Thus, if there is no precise knowledge of disturbance, then the full benefits of STSM cannot be achieved for improving the control performance.

To address this drawback, it has been suggested to incorporate the super-twisting sliding mode (STSM) control design together with a disturbance observer (DOB). The DOB provides online estimation of the total system disturbances and feedbacks it to the STSM controller to reject the disturbances impacting the system performance [18]. Out of the various disturbance observation approaches, the extended state observer (ESO) has received much consideration because it can handle the estimation of system states and disturbances for improved control performance [19]. However, classical ESO method guarantee that the estimation error converges to zero asymptotically, which is not suitable for fast disturbance reference signals, as the estimation accuracy deteriorates . To overcome this restriction, the notion of finite-time control (FTC) was introduced, and the finite-time extended state observer (FTESO) and its application were presented [20]. The main benefit of the FTESO is that it guarantees the convergence of the estimation error to zero in a finite time, which results in faster response times and better accuracy [21]. These properties are very useful for control systems that have strict real-time performance

*e-mail: liyong@ujs.edu.cn

demands, for instance, high-precision speed control in PMSM drive systems. Based on this, Qiankang Hou et al. proposed an STSM coupled with FTESO for the control of PMSM drive systems to achieve better disturbance rejection and tracking performance [22]. Likewise, Wei Xu et al. proposed a composite speed control strategy based on the finite-time sliding mode observer (FTSMO)[23]. This method uses the FTSMO to online identify system disturbances and counteracts them through a feedforward action to enhance the system robustness and dynamic performance.

The research findings reveal that the integration of the finite-time extended state observer (FTESO) with the super-twisting sliding mode controller (STSM) significantly enhances the ability of disturbance rejection and control stability of the PMSM system under challenging conditions, such as load torque variations and rotational inertia fluctuations. Building on these findings, this paper proposes a novel composite control strategy that combines the finite-time sliding mode observer (FTSMO) with the super-twisting sliding mode controller (STSM). The proposed strategy is rigorously validated through both simulations and experimental studies within the PMSM drive system. The results demonstrate that the proposed control approach effectively improves the anti-disturbance capability, tracking precision, and robustness of the PMSM system, thereby optimizing its dynamic response and steady-state performance.

This paper is structured in the following way: Section II given the mathematical modeling of the PMSM system and presents the traditional composite control approach that utilizes the ESO. Section III outlines the suggested composite control strategy based on super-twisting sliding mode, which includes the finite-time extended state observer, and presents a thorough stability analysis. Section IV demonstrates the effectiveness of the proposed control approach via experimental research and offers an in-depth analysis of the findings. In conclusion, Section V wraps up the study by highlighting the main discoveries and provides a brief discussion on possible future research avenues.

2. PERMANENT MAGNET SYNCHRONOUS MOTOR SYSTEM MODELLING

2.1. Basic model of permanent magnet motor

Considering the dynamic equations of a permanent magnet synchronous motor (PMSM), the overall mechanical equations of motion can be formulated as follows:

$$\dot{\omega} = \frac{3}{2} \frac{n_p \psi_f}{J} i_q - \frac{B}{J} \omega - \frac{T_L}{J} \qquad (1)$$

In this expression, ω denotes the mechanical rotor speed, $\dot{\omega}$ represents the angular acceleration, n_p is the number of pole pairs, ψ_f is the permanent magnet flux linkage, J is the rotational inertia, i_q is the q-axis current, B is the viscous friction coefficient, and T_L is the load torque. By replacing unknown disturbances (e.g., those from load torque and friction) with the lumped disturbance term $d(t)$, the system dynamics are refor-
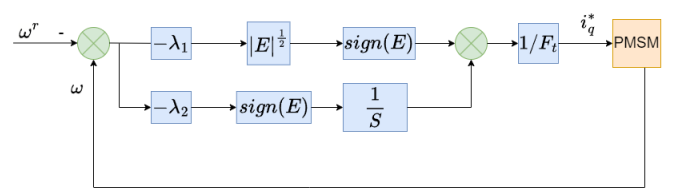

Fig. 1. STSM controller

mulated as follows:

$$\dot{\omega} = F_t i_q + d(t) \qquad (2)$$

where $F_t = \frac{3n_p \psi_f}{2J}$ and $d(t) = -\frac{B}{J}\omega - \frac{n_p}{J}T_L$. In the actual control system, $-\frac{B}{J}\omega$ and $-\frac{n_p}{J}T_L$ represent unknown disturbances or uncertainties in the system, which may be caused by load variations, parameter changes, or environmental influences.

To guarantee the reliability of the motion control system, it is essential to estimate and adjust for these disturbances in real time. This paper's goal is to create a composite control law that guarantees rapid convergence of the velocity tracking error.

2.2. The Structure of the STSM Controller

The super-twisting sliding mode (STSM) control algorithm, recognized for its robust anti-disturbance capabilities, is implemented in this study. Initially introduced by A. Levant in [24], the STSM algorithm constitutes an advanced sliding mode control methodology distinguished by its straightforward architecture and superior disturbance rejection performance. A key advantage of the STSM algorithm lies in its ability to smooth discontinuous signals, thereby improving the continuity of the control process compared to traditional first-order sliding mode controllers. the super-twisting sliding mode control law is designed as follows:

$$i_q^* = -\frac{1}{F_t} \left(\lambda_1 |E|^{\frac{1}{2}} \operatorname{sign}(E) + \lambda_2 \int \operatorname{sign}(E) dt \right) \qquad (3)$$

the system q-axis current reference is denoted by i_q^*. The control gains, represented by λ_1 and λ_2, determine the convergence speed of the system. The reference speed intended for the system is represented by ω_r. To guarantee that the speed error E diminishes to zero within a finite time, the design of i_q^* is structured to allow the rotor speed ω to effectively follow the reference speed ω_r. The stability properties and finite-time convergence characteristics of the Second-order Tracking-Sliding Mode (STSM) controller were rigorously proven through comprehensive theoretical analysis and experimental validation, as demonstrated in [25]. The controller system's block diagram is shown in Fig. 1.

2.3. The composite controller is based on STSM

As demonstrated in the actual control system, as expressed in equation (2), The existence of the lumped disturbance term considerably affects the overall performance of the system. As a result, it is necessary to include disturbance compensation. Accordingly, the composite control law is formulated as follows:

2

$$\mathrm{i}_q^* = -\frac{1}{F_t}\left(\lambda_1|E|^{\frac{1}{2}}\operatorname{sign}(E)+\lambda_2\int\operatorname{sign}(E)dt+\hat{d}(t)\right)\text{(4)}$$

where, $\hat{d}(t)$ is an estimate of the actual perturbation $d(t)$. if the observer can provide an accurate estimate, no scaling factor is required.

λ_1 is responsible for quickly pulling the system back when the state deviates from the sliding mode surface. It typically needs to be sufficiently large to ensure fast convergence speed and robustness, but being too large can amplify the impact of measurement noise, so it must be adjusted based on the system's desired dynamic response speed. λ_2 is responsible for real-time estimation and compensation of various internal and external uncertainties in the system, enabling the system to move smoothly and continuously along the sliding surface once it reaches it, thereby avoiding the chattering caused by high-frequency switching in traditional sliding mode control. However, if λ_2 is too small, it cannot effectively suppress strong disturbances, leading to performance degradation or even instability. If it is too large, although robustness is enhanced, it may result in excessive control actions and increased sensitivity to noise. This paper primarily uses theoretical guidance to first determine λ_1 through multiple experiments, then adjust λ_2 while ensuring good response, enabling it to quickly recover to steady state under conditions such as load changes and maintain minimal overshoot throughout the process. The combination of the two ensures that the STSM controller exhibits strong robustness against changes in motor parameters (such as resistance and inductance), changes in rotational inertia, and load torque disturbances, while maintaining excellent dynamic response performance. Under certain conditions, the STSM ensures that the system state converges precisely to the sliding mode surface within a finite time and remains on it.

In this paper, a comparative analysis is conducted between the conventional ESO-STSM composite controller and the proposed FTSMO-STSM composite strategy. Specifically, the traditional ESO estimates the lumped disturbance $d(t)$ and feeds it forward into the STSM control law (Eq. (3)) to form an ESO-based composite controller . This integration aims to synergize ESO's disturbance estimation with STSM's robustness. The STSM-ESO method, detailed in [22], serves as the benchmark for experimental validation. However, the ESO guarantees only *asymptotic* convergence of estimation errors (i.e., $\hat{d}(t)\to d(t)$ as $t\to\infty$), leading to slower convergence and limited accuracy under rapid disturbances. Given PMSM's susceptibility to parameter uncertainties, load variations, and nonlinearities, this delay compromises tracking precision and robustness.

To address this, we propose replacing ESO with a Finite-Time Sliding Mode Observer (FTSMO). The FTSMO leverages a generalized super-twisting structure (Eq. (5)) to ensure estimation errors converge to zero *in finite time*, significantly accelerating convergence and improving accuracy. This enhancement directly boosts the dynamic response and robustness of the composite STSM-FTSMO controller.

3. COMPOSITE CONTROL STRATEGIES PROPOSED

The core advantage of the STSM controller lies in its strong anti-interference capability, ability to converge within a limited time, and simple parameters that are easy to adjust. FTSMO can accurately estimate unknown disturbances within a limited timeframe and promptly compensate for system disturbances, thereby significantly enhancing the system's interference resistance. Theoretically, the composite control framework based on STSM and FTSMO has the ability to improve dynamic response, utilize FTSMO's feedforward compensation to reduce overshoot, and maintain excellent interference resistance after system disturbances, making it particularly suitable for scenarios with stringent control performance requirements.

3.1. The FTSMO observer

The real-time estimation of unknown disturbances, including load perturbations and parameter perturbations, is performed using a FTSMO as follows.

$$\begin{cases} \dot{\hat{\omega}}=\frac{3}{2}\frac{n_p}{J}\psi_f i_q-\frac{B}{J}\hat{\omega}+l_o \\[2mm] l_o=-m_o k^{1/3}|\hat{\omega}-\omega|^{2/3}\cdot\operatorname{sign}(\hat{\omega}-\omega)+\hat{d}(t) \\[2mm] \dot{\hat{d}}(t)=-m_1 k^{1/2}|\hat{d}(t)-l_o|^{2/3}\cdot\operatorname{sign}(\hat{d}(t)-l_o)+l_1 \\[2mm] \dot{l}_1=-m_2 k\cdot\operatorname{sign}(l_1-\dot{\hat{d}}(t)) \end{cases}\text{(5)}$$

where, $\hat{\omega}$ is the rotor speed estimation, $\dot{\hat{\omega}}$ is the derivative of the estimated speed. l_o is the disturbance estimation intermediate variable, $\hat{d}(t)$ is the system estimation disturbance, $\dot{\hat{d}}(t)$ is the derivative of the estimated disturbance. m_o and k are observation gains whose values are adjusted according to the system operating effects. It can be shown that the configuration of the multilayer perturbation estimation guarantees the convergence of the perturbation estimation within a finite time frame. In this structure, m_1 and m_2 represent the control gains of the observer, and l_1 is a higher-order variable that enhances the finite-time convergence property.

As evidenced by equations(5) , the parameter selection of k, m_0, m_1, and m_2 constitutes a critical factor in determining the system performance when implementing a finite-time sliding mode observer (FTSMO). Parameter m_0 dominates speed error convergence (affecting response speed), parameter m_1 smoothes disturbance estimation (suppressing noise), and m_2 compensates for disturbance derivatives (resistance to sudden changes). This paper adopts an engineering experimental method, first fixing k to a constant value, adjusting m_0 so that the system can quickly reach the response, and then adjusting m_1 and m_2 on this basis to first obtain parameters that allow the system to operate normally, and then fine-tuning them to achieve better dynamic response and disturbance recovery performance. Through systematic optimization of the switching gain, the system convergence time can be significantly reduced. Nevertheless, an excessively high FTSMO gain may

3

lead to pronounced overshooting in the velocity response, consequently compromising the steady-state accuracy of the system. Therefore, precise estimation of the total disturbance during the compensation process emerges as a crucial requirement for maintaining system robustness. In conclusion, the strategic parameter configuration represents a fundamental aspect for achieving enhanced control performance and robust system operation.

3.2. Stability analysis of the FTSMO

This study offers a thorough theoretical examination of the finite-time convergence properties for the suggested Finite-Time Sliding Mode Observer (FTSMO) utilized in permanent magnet synchronous motor (PMSM) drive systems. The stability analysis is established through a hierarchical composite Lyapunov function methodology, building upon the theoretical frameworks developed in [26, 27]. The observer architecture integrates advanced finite-time differentiation techniques derived from sliding mode differentiators [28]. By conducting theoretical analysis and selecting appropriate gains, it has been mathematically established that the dynamics of observer error can converge to zero asymptotically within a finite timeframe [29], demonstrating the effectiveness of the proposed approach.

The system dynamics are characterized by defining ω as the actual angular velocity, with $\hat{\omega}$ and $\hat{d}(t)$ representing the observer's estimates of the angular velocity and lumped disturbance term $d(t)$, respectively. The estimation error dynamics are formally defined through the following state variables:

$$e_1 = \hat{\omega} - \omega, \quad e_2 = \hat{d}(t) - d(t), \quad e_3 = \dot{\hat{d}}(t) - \dot{d}(t). \quad (6)$$

The theoretical development of the proposed methodology is based on the following fundamental assumptions:

Assumption 3.1 (Regularity of the System States) *The system states (e.g., ω and the current i_q) are continuously differentiable, and their derivatives are Lipschitz continuous with Lipschitz constant $N > 0$ [30].*

Assumption 3.2 (Bounded Disturbance) *The lumped disturbance $d(t)$ and its derivative $\dot{d}(t)$ are both limited; specifically, there is a constant $N > 0$ such that:*

$$|\dot{d}(t)| \leq N, \quad \forall t \geq 0.$$

Based on the observer design [23] and the finite-time differentiator techniques introduced in [28], The dynamics of the error can be represented as:

$$\dot{e}_1 = -\frac{B}{J}e_1 - m_0 k^{\frac{1}{3}}|e_1|^{\frac{2}{3}}\mathrm{sgn}(e_1) + e_2, \quad (7)$$

$$\dot{e}_2 = -m_1 k^{\frac{1}{2}}|e_2 - \dot{e}_1|^{\frac{1}{2}}\mathrm{sgn}(e_2 - \dot{e}_1) + e_3, \quad (8)$$

$$\dot{e}_3 \in -m_2 k\,\mathrm{sgn}\left(e_3 - (e_2 - \dot{e}_1)\right) + d, \quad |d| \leq N. \quad (9)$$

To simplify notation, define:

$$\delta_2 = e_2 - \dot{e}_1, \quad \delta_3 = e_3 - \delta_2.$$

The proof of stability is established by creating the subsequent candidate Lyapunov function:

$$V_1 = \frac{1}{2}e_1^2, \quad V_2 = \frac{1}{2}\delta_2^2, \quad V_3 = \frac{1}{2}\delta_3^2,$$

and the overall composite Lyapunov function as:

$$V = V_1 + V_2 + V_3.$$

Step 1: $\dot{V}_1$

From the dynamics:

$$\dot{e}_1 = -\frac{B}{J}e_1 - m_0 k^{1/3}|e_1|^{2/3}\mathrm{sgn}(e_1) + e_2 \quad (10)$$

Then:

$$\dot{V}_1 = e_1\dot{e}_1 \quad (11)$$

$$= -\frac{B}{J}e_1^2 - m_0 k^{1/3}|e_1|^{5/3} + e_1 e_2 \quad (12)$$

Apply Young's inequality:

$$|e_1 e_2| \leq \frac{m_0 k^{1/3}}{2}|e_1|^{5/3} + \frac{1}{2m_0 k^{1/3}}|e_2|^5 \quad (13)$$

So:

$$\dot{V}_1 \leq -c_1|e_1|^{5/3} + C_1|e_2|^5 \quad (14)$$

Step 2: $\dot{V}_2$

$$\dot{e}_2 = -m_1 k^{1/2}|\delta_2|^{2/3}\mathrm{sgn}(\delta_2) + e_3 \quad (15)$$

$$\dot{\delta}_2 = \dot{e}_2 - \ddot{e}_1 \quad (16)$$

Then:

$$\dot{V}_2 = \delta_2\dot{\delta}_2 \leq -c_2|\delta_2|^{3/2} + C_2|e_3|^r \quad (17)$$

Step 3: $\dot{V}_3$

From the dynamics:

$$\dot{e}_3 = -m_2 k\,\mathrm{sgn}(\delta_3) + d(t) \quad (18)$$

$$\dot{V}_3 = \delta_3\dot{e}_3 \leq -(m_2 k - N)|\delta_3|, \quad \text{if } m_2 k > N \quad (19)$$

The primary objective of this analysis is to demonstrate the existence of positive constants $c > 0$ and $\alpha \in (0,1)$ satisfying the following condition:

$$\dot{V} \leq -cV^\alpha,$$

According to finite-time stability theory [26, 29], this implies that $V(t)$ will reach zero in finite time:

$$T \leq \frac{V(0)^{1-\alpha}}{c(1-\alpha)} \quad (20)$$

which leads to the conclusion that the errors e_1, e_2, and e_3 will converge to zero within a finite time period.

4

Lemma 3.1 *Consider the error dynamic* (7). *If the gain* m_0 *and constant* k *are chosen sufficiently large such that the term* $-m_0 k^{\frac{1}{3}} |e_1|^{\frac{5}{3}}$ *dominates the cross-term* $e_1 e_2$, *then the time derivative of* V_1 *satisfies:*

$$\dot{V}_1 \leq -c_1 |e_1|^{\frac{5}{3}} + C_1 |e_2|^q,$$

for some constants $c_1 > 0$, $C_1 > 0$, *and exponent* $q > 0$.

Differentiating V_1 along (7) yields:

$$\dot{V}_1 = e_1 \dot{e}_1 = -\frac{B}{J} e_1^2 - m_0 k^{\frac{1}{3}} |e_1|^{\frac{5}{3}} + e_1 e_2.$$

Applying Young's inequality to the cross-term $e_1 e_2$, one obtains an estimate of the form:

$$|e_1 e_2| \leq \frac{m_0 k^{1/3}}{2} |e_1|^{5/3} + \frac{1}{2 m_0 k^{1/3}} |e_2|^5 \qquad (21)$$

which leads to the stated bound.

Lemma 3.2 *For the error dynamic* (8) *with* $\delta_2 = e_2 - \dot{e}_1$, *if the gain* m_1 *and constant* k *are appropriately selected, then the derivative of* V_2 *satisfies:*

$$\dot{V}_2 \leq -c_2 |\delta_2|^{3/2} + C_2 |e_3|^r,$$

with constants $c_2 > 0$, $C_2 > 0$, *and* $r > 0$.

Differentiate δ_2 to obtain

$$\dot{\delta}_2 = \dot{e}_2 - \ddot{e}_1.$$

The term $-m_1 k^{\frac{1}{2}} |\delta_2|^{\frac{1}{2}} \operatorname{sgn}(\delta_2)$ provides sufficient damping. By bounding the coupling terms (including $\ddot{e}_1$ and e_3) via Youngs inequality, the stated inequality follows [27].

Lemma 3.3 *For the error dynamic* (9) *with* $\delta_3 = e_3 - \delta_2$, *if the gain* m_2 *and constant* k *satisfy*

$$m_2 k > N,$$

then the derivative of V_3 *satisfies*

$$\dot{V}_3 \leq -(m_2 k - N)|\delta_3|.$$

From (9), we have:

$$\dot{e}_3 \in -m_2 k \operatorname{sgn}(\delta_3) + d, \quad |d| \leq N. \qquad (22)$$

Multiplying by δ_3 gives:

$$\delta_3 \dot{e}_3 \leq -m_2 k |\delta_3| + N |\delta_3| = -(m_2 k - N)|\delta_3| \qquad (23)$$

which implies the stated bound.

Theorem 3.1 *Consider the observer error dynamics given in* (7)–(9) *and assume that Assumptions 3.1 and 3.2 hold. If the observer gains* m_0, m_1, m_2 *and the constant* k *are chosen such that:*

- $m_0 k^{\frac{1}{3}}$ *is sufficiently large to dominate the cross-term in* $\dot{V}_1$,
- m_1 *and* k *are chosen to ensure* $\dot{V}_2 \leq -c_2 |\delta_2|^{\frac{3}{2}} + C_2 |e_3|^r$,
- $m_2 k > N$

then there exist constants $c > 0$ *and* $\alpha \in (0, 1)$ *such that the composite Lyapunov function satisfies*

$$\dot{V} \leq -cV^\alpha \qquad (24)$$

As a result, the observer errors e_1, e_2, and e_3 diminish to zero within a finite period of time [26, 29].

3.3. Composite control strategy of STSM and FTSMO

In order to enhance the system's capacity to anti-disturbances, this paper proposes a composite control strategy that integrates super-twisting sliding mode control (STSM) and finite time sliding mode observer (FTSMO). Within this control framework, accurate estimation of the lumped disturbance is crucial for the effective compensation of the disturbance. The implementation of the feedforward compensation method can additionally lessen the impact of disturbances and enhance both the dynamic response and steady-state performance of the system. The architectural structure of the suggested FTSMO-based STSM composite control strategy is depicted in Fig. 2. To enable the analysis that follows, the dynamics of the error are defined as such:

$$\begin{aligned} E_1 &= \hat{\omega} - \omega, \\ E_2 &= \hat{d}(t) - l_o, \\ E_3 &= l_1 - \dot{\hat{d}}(t), \end{aligned}$$

where E_1, E_2, and E_3 represent the state estimation errors for angular velocity, disturbance observation, and auxiliary state variable, respectively. The proposed STSM+FTSMO composite controller is an outer-loop controller and the primary control loop. It handles speed error (the difference between the reference speed ω^* and the actual measured speed ω) and generates the q-axis current reference value (i_q^*). FTSMO plays a crucial role here, with its input being the actual q-axis current iq and the actual measured speed , and its output being the estimated disturbance. It can perform real-time, finite-time precise estimation of superimposed disturbances, including external load torque and internal parameter changes. The estimated disturbances are then fed into the STSM controller for active compensation, thereby enhancing robustness and dynamic response. The STSM controller and FTSMO observer work together to achieve excellent control performance and effective disturbance suppression. The proposed STSM+FTSMO composite controller is an outer-loop controller and the primary control loop. It handles speed error (the difference between the reference speed ω^* and the actual measured speed ω) and generates the q-axis current reference value i_q^*. The FTSMO plays a crucial role here, with its inputs being the actual q-axis current iq and the actual measured speed , and its output being the estimated disturbance. It can perform real-time, finite-time precise estimation of superimposed disturbances, including external load torque and internal parameter changes. The estimated disturbances are then fed into the STSM controller for active compensation, thereby enhancing robustness and dynamic response. The STSM controller and FTSMO observer work together to achieve excellent control performance and effective disturbance suppression. The structure outside the composite controller aligns with the traditional PI internal current loop and external speed loop control strategy, the rated current of the motor is 6A, and the instantaneous current limit value i_q^* is 3.5 times the rated value. as detailed in Figure 2.
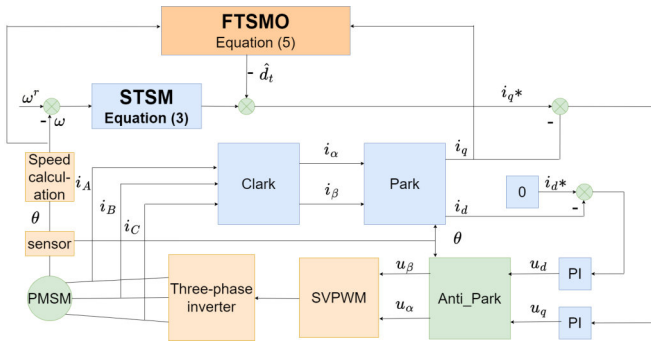
5

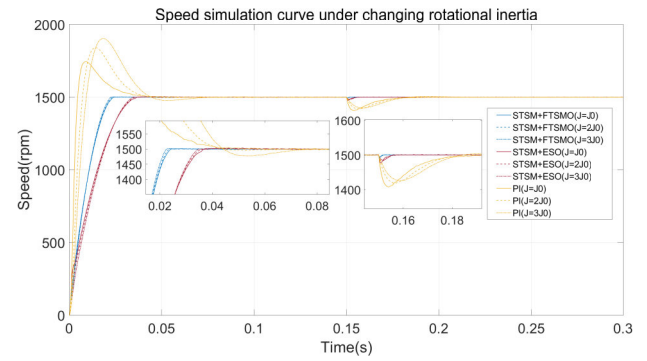**Fig. 2.** Composite control strategy of STSM and FTSMO

Fig. 3. Simulation of speed performance under changing rotational inertia

4. SIMULATION VERIFICATION

To verify that the algorithm proposed in this paper still exhibits disturbance suppression performance after changing system parameters, three algorithms STSM+FTSMO, STSM+ESO, and PI were used as the outer loop to construct a PMSM control system in MATLAB simulation software. The three algorithms were tested under three different rotational inertia conditions: $J = J_0 = 0.2 \times 10^{-2} \text{kg} \cdot \text{m}^2$, $J = 2J_0$, and $J = 3J_0$, with all other module parameters kept consistent. Start-up and loading experiments were conducted under these conditions. The resulting speed curves are shown in 3. The solid line represents the curve for a rotational inertia of $J = J_0$, the dashed line represents the curve for a rotational inertia of $J = 2J_0$, and the dashed-solid line represents the curve for a rotational inertia of $J = 3J_0$. From the solid-line velocity curves ($J = J_0$) of the three algorithms, it can be seen that the STSM+FTSMO and STSM+ESO algorithms outperform the traditional PI algorithm in terms of the time to reach steady state after startup and reducing overshoot. Additionally, the STSM+FTSMO algorithm reaches steady state faster than the STSM+ESMO algorithm after startup and maintains a smoother velocity once steady state is achieved. When the same load is applied after 0.15 seconds of simulation time, STSM+FTSMO performs better than STSM+ESO in terms of speed drop and recovery time, and significantly outperforms traditional PI, consistent with the results obtained from experiments on a motor test bench. Under the same simulation conditions, the rotational inertia was increased by $2J_0$ and $3J_0$, respectively. As shown in the simulation diagram, increasing the rotational inertia by three times caused the PI to exhibit greater overshoot and a longer time to reach steady state. After loading, due to changes in rotational inertia, the speed curve changed significantly. However, the STSM+FTSMO and STSM+ESO algorithms, which employ feedforward observers to compensate for changes in system parameters, also suppress overshoot. Despite the rotational inertia increasing by a factor of two during startup and loading, the overall speed curve changes are not prominent. Through this simulation, it can be seen that the STSM+FTSMO algorithm also performs very well under conditions of a threefold change in rotational inertia, indicating that the STSM+FTSMO composite controller has a suppressing effect on disturbances caused by changes in rotational inertia.

5. EXPERIMENTAL VERIFICATION

In order to confirm the theoretical framework and assess the practical effectiveness of the proposed control approach, comprehensive real-time experimental studies were conducted. The experimental configuration, schematically illustrated in Fig. 4, incorporates a dual-motor test bench equipped with two 1.8 kW permanent magnet synchronous motors (PMSMs). The system is governed by a high-performance control platform based on the TMS320F28379D digital signal processor (DSP), which facilitates precise real-time implementation of advanced control algorithms. In this architecture, the primary motor operates as the controlled plant, while the secondary motor serves as the load emulator to replicate dynamic operational conditions. In this configuration, the primary motor implements the proposed control algorithm, while the secondary motor serves as a dynamically controlled load unit, enabling precise emulation of various load torque conditions. This experimental arrangement facilitates rigorous evaluation of the control strategy's dynamic characteristics and disturbance rejection capabilities under realistic operating conditions. The comprehensive technical details of the experimental PMSM drives can be found in Table 1.
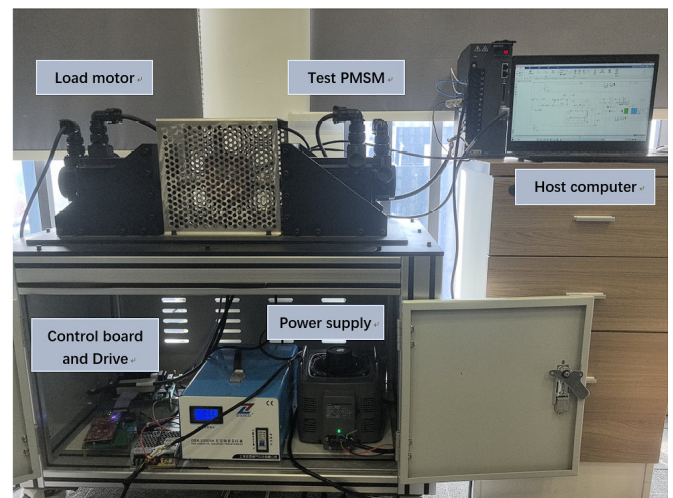

Fig. 4. Experimental bench

To comprehensively assess the efficacy of the control strate-

Table 1. Experimental motor parameters

Parameters	Symbol	Value
Rated power	p	1.8 kW
Stator resistance	R_s	0.81 Ω
Mutual inductance	L_s	2.59 mH
Inertia	J	$0.76 \times 10^{-3} kg \cdot m^2$
Flux linkage	Ψ_f	0.117 Wb

Table 2. Motor algorithm control parameters

Parameters of controllers	Values and Units
Sampling frequency	10 kHz
PI gains	KP=0.09 , KI=0.3
The gains of STSM+ESO	λ_1=300,λ_2=1200, ζ_1=1600,ζ_2=80
The gains of STSM+FTSMO	λ_1=300,λ_2=1200, m_0=600,m_1=300, m_2=12,K=120

gies, three algorithms were experimentally validated under various operating conditions: conventional Proportional-Integral (PI) control, Super-Twisting Mode (STSM) control combined with an Extended State Observer (ESO) (denoted as STSM+ESO), and Super-Twisting Sliding Mode (STSM) control combined with a Finite Time Sliding Mode Observer (FTSMO) (denoted as STSM+FTSMO). The key variables associated with each control strategy were compared and analyzed. The experimental results indicate the variations in performance among the control methods under various operating conditions, and their steady-state accuracy along with dynamic response were thoroughly assessed. The parameters employed in the three algorithms are listed in Table 2. To guarantee an equitable comparison, the STSM controller utilized in the composite controllers applied the same parameters.where ζ_1 and ζ_2 are the gains of the ESO.

5.1. Start-up transient and steady-state performance analysis under no-load conditions

The transient response characteristics of the conventional PI controller, the Second-order Tracking-Sliding Mode (STSM) controller integrated with an Extended State Observer (ESO), and the STSM controller augmented with a Fast Terminal Sliding Mode Observer (FTSMO) are comparatively analyzed in Fig. 5 and Fig. 6 . These evaluations were conducted under unloaded operational conditions with reference speeds set to 800 rpm and 1500 rpm, respectively, to examine the controllers initial dynamic performance during speed step transitions.From the experimental results, it can be observed that the traditional PI controller has a fast start-up response without output constraints, but there is a significant overshoot phenomenon and it takes a long time to reach the steady state control. In contrast, the STSM+ESO and STSM+FTSMO exhibit considerable differences in both steady-state response and dynamic performance due to the same controller architecture, the same parameter settings, and only the difference in observer design.

As shown in Fig. 5, which compares the three algorithms, the STSM+FTSMO and STSM+ESO algorithms exhibit virtually no overshoot at an 800 rpm setpoint. This is attributed to the effective suppression of overshoot achieved by combining the STSM controller with the feedforward observer. The time taken for the STSM+FTSMO, STSM+ESO, and PI algorithms to reach steady-state speed is 79 ms, 229 ms, and 300 ms, respectively. This demonstrates that the combination of the FTSMO observer and STSM controller achieves a faster response speed than STSM+ESO, with a steady-state time that is 3.5 times faster than traditional PI control. In Fig. 6, when the speed setpoint is 1500 rpm, the performance of the three algorithms is similar to that in Fig. 5, with steady-state times of 101 ms, 320 ms, and 495 ms. Moreover, under this condition, there is no notable difference between the q-axis current and the a-phase current, indicating that this control strategy can maintain more stable current characteristics during the start-up phase.

This experimental result verifies the advantages of the STSM+FTSMO control algorithm in motor start-up response time optimisation and overshoot suppression. By comparing the speed waveforms of the three control strategies, it is evident that the STSM+FTSMO achieves steady state more quickly and with almost no overshoot in contrast to the PI controller. Meanwhile, compared to STSM+ESO, it has a faster response speed and a shorter rise time, which allows the system to reach the set speed value faster, thereby demonstrating dominance in both transient and steady-state performance.

### 5.2. Anti-disturbance performance analysis of the drive system

Figures 7 and 8 illustrate the changes in speed response, q-axis current, and a-phase current for the three different control strategies: PI control, STSM+ESO, and STSM+FTSMO, when a load of 1.8 N.m is applied at reference speeds of 800 rpm and 1500 rpm, respectively. The experimental results indicate that all three control strategies exhibit a certain degree of speed fluctuation following the application of the load at 2.9s.

However, compared to the PI controller, STSM+ESO and STSM+FTSMO demonstrate superior resistance to load disturbances. In Figures 7, when the set speed is 800 rpm, the instantaneous speed drops of the STSM+FTSMO, STSM+ESO, and PI algorithms during load application are 43 rpm, 75 rpm, and 103 rpm, respectively, while the steady-state recovery times are 59 ms, 121 ms, and 252 ms, respectively. In Figures 8, when the set speed is 1500 rpm, due to the high speed and large system inertia, the speed drops are not significantly different, at 45 rpm, 65 rpm, and 65 rpm, respectively, with steady-state recovery times of 72 ms, 151 ms, and 412 ms. From the experimental results, it can be seen that, thanks to the combination of an excellent controller and a feedforward observer, the STSM+FTSMO system demonstrates superior performance in terms of dynamic recovery capability after system disturbances. Notably, under identical controller structures and parameters, the STSM+FTSMO system is more effective than the STSM+ESO system in mitigating the impact of load dis-
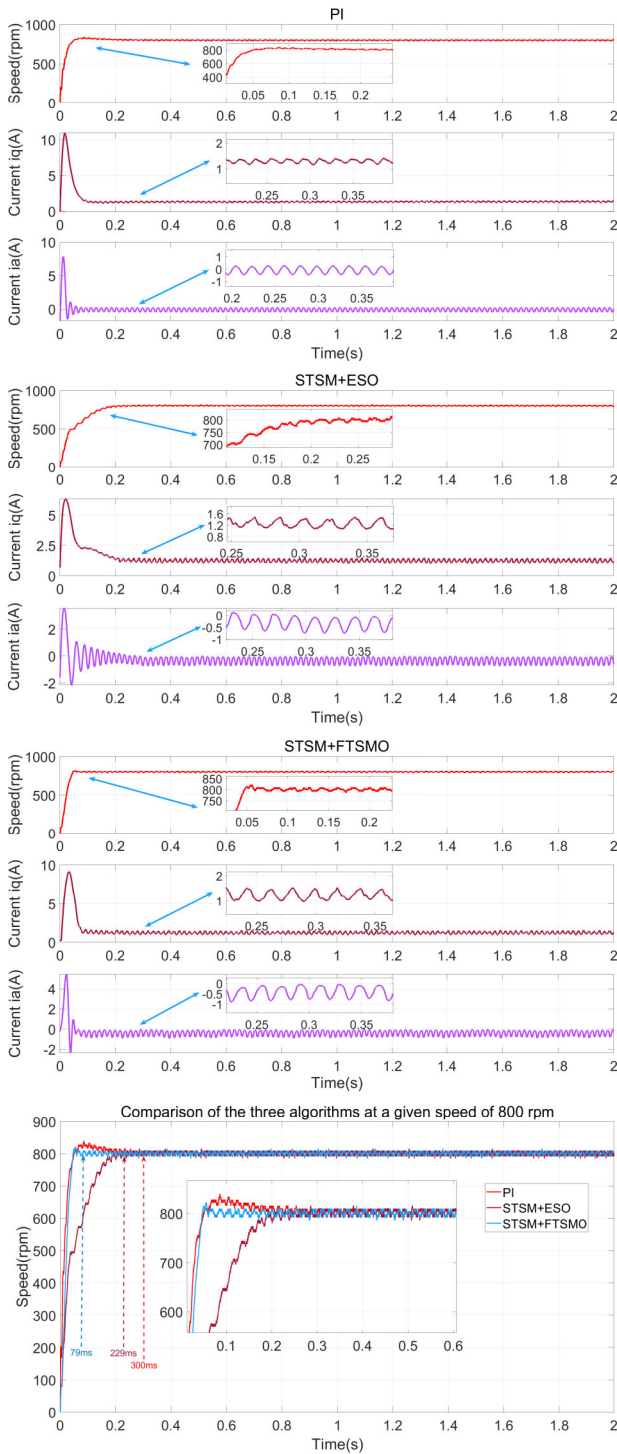
Fig. 5. Comparison of variables at startup of the three algorithms when the set value is 800rpm
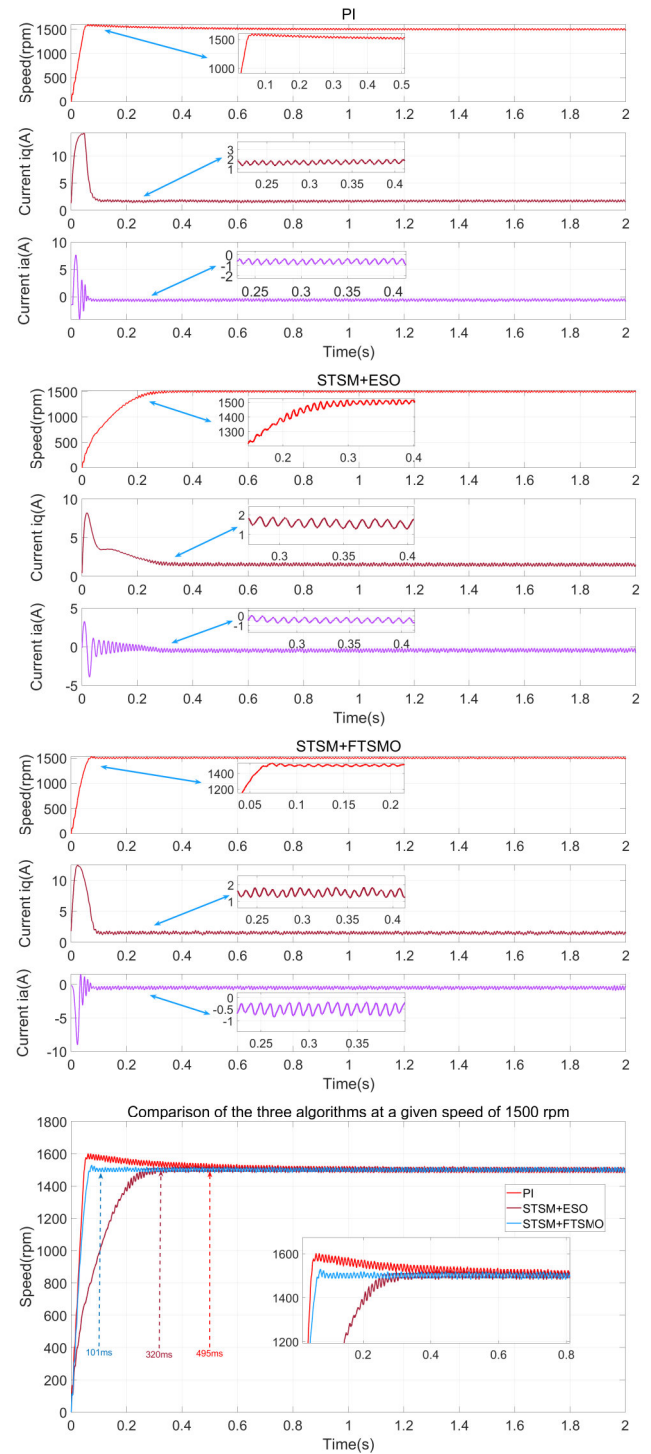
Fig. 6. Comparison of variables at startup of the three algorithms when the set value is 1500rpm

turbances, and there are no significant differences in the q-axis current and a-phase current. Overall, STSM+FTSMO outperforms the other two control strategies in terms of disturbance suppression and steady-state recovery time, thereby confirming its control advantages in complex load environments.

5.3. Reversing performance over the entire speed range

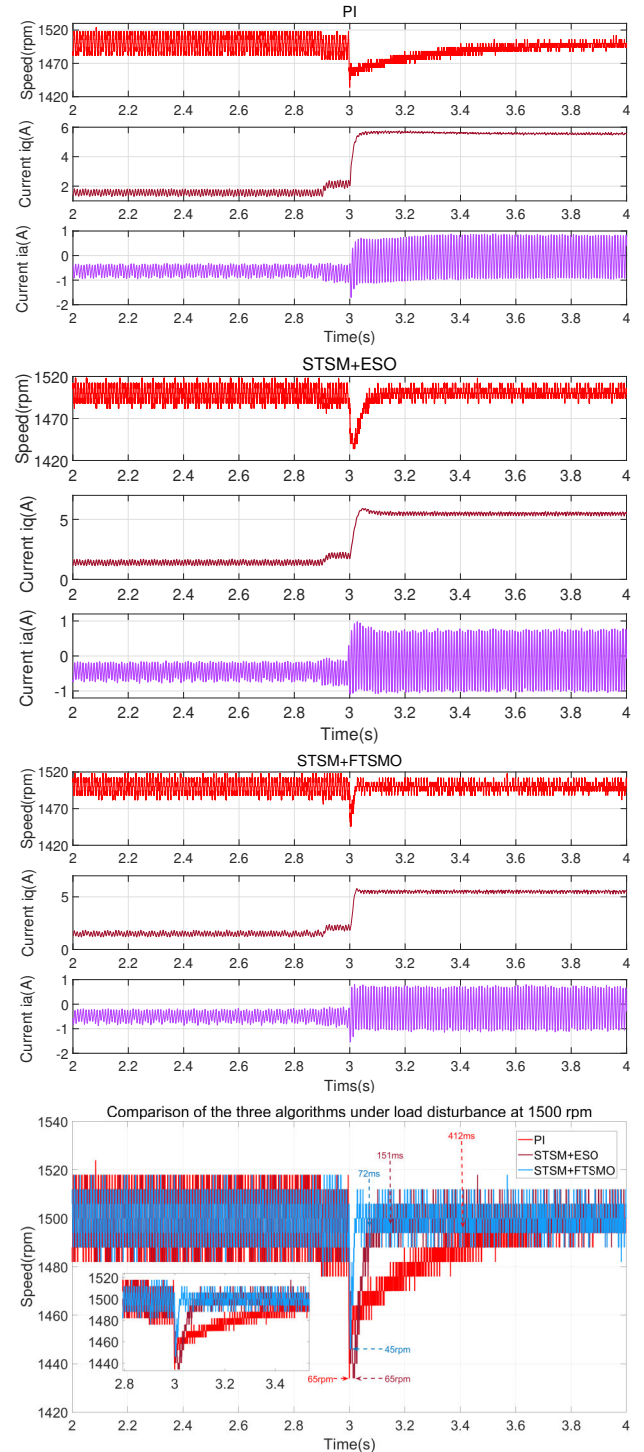To verify the performance of STSM+FTSMO across the en-

tire speed range, speed reversal experiments were conducted at low speeds of 300 rpm, 600 rpm, and 1000 rpm, and at medium-high speeds of 1500 rpm, 2000 rpm, 2500 rpm, and 3000 rpm. The experiments captured three forward and reverse cycles totaling 9 seconds. As shown in Figure 9, the q-axis current corresponding to different speeds is displayed below the speed reversal experiment graph, with the color of a specific speed curve matching that of the corresponding cur-

8
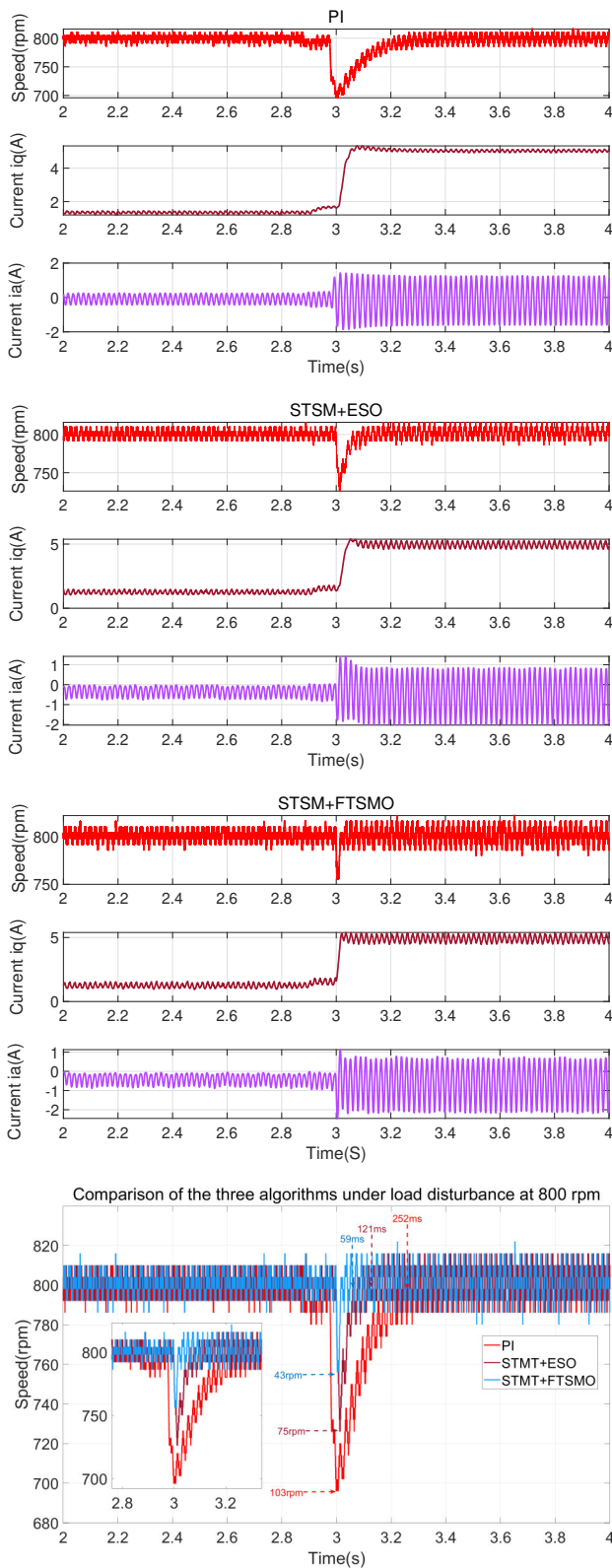
Fig. 7. Performance of three algorithms under a load of 1.8 N at a speed of 800 rpm

Fig. 8. Performance of three algorithms under a load of 1.8 N at a speed of 1500 rpm

rent curve. From the low-speed reversal speed graph, it can be seen that under no-load conditions, the transition from -1000 rpm to 1000 rpm and reaching steady-state takes only 116 ms,

with virtually no overshoot. For the 300 rpm and 600 rpm reverse experiments, the figure shows that the time to reach steady state is even shorter. The corresponding low-speed reverse current curve reaches its maximum value at the moment of startup and quickly stabilizes. Similarly, in the medium-high speed reverse speed diagram, the speed reaches steady state from -3000 rpm to 3000 rpm in approximately 210 ms. Other medium-high speed reversals reach steady state in less

9

than 210 ms. The corresponding instantaneous current values at startup are close to the set limit values, enabling the motor to quickly enter steady state and rapidly decrease to the system's stable operating platform value, with minimal overshoot. Throughout the experiment, it can be observed that the STSM+FTSMO algorithm demonstrates excellent performance across the entire speed range, resulting in motors that not only exhibit minimal overshoot but also achieve steady-state quickly and operate smoothly.
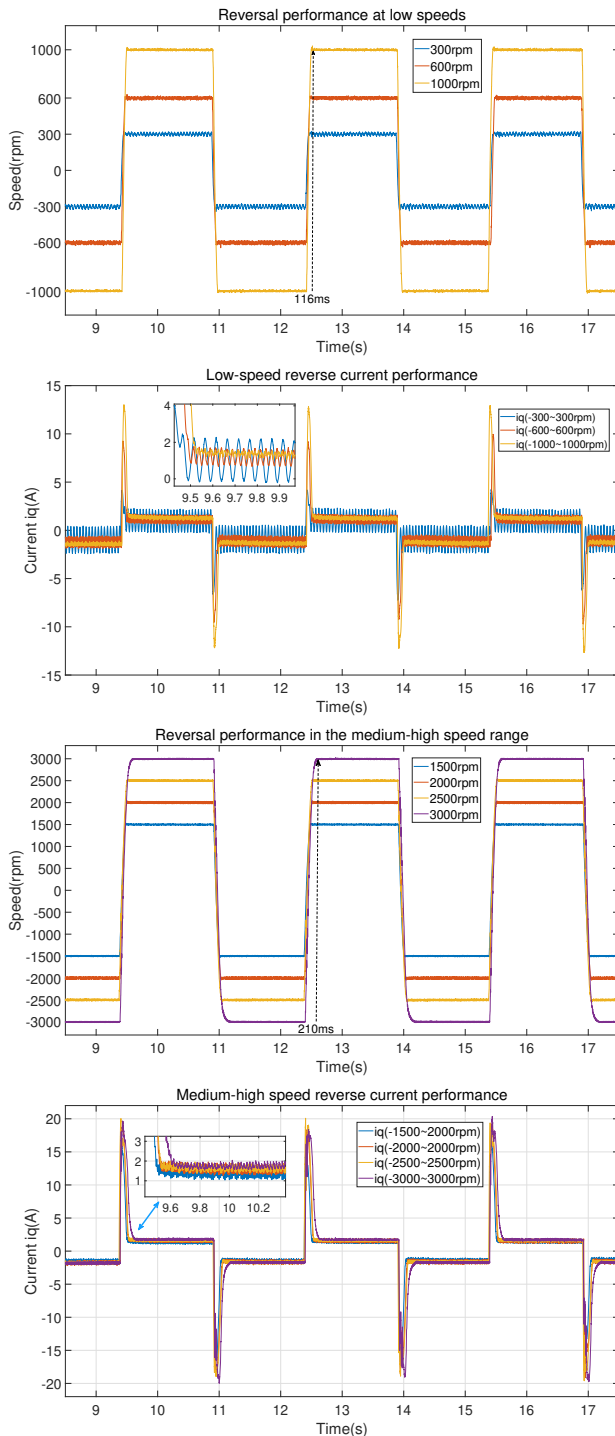

Fig. 9. Reversing performance over the entire speed range

6. CONCLUSION

This paper introduces a high-performance composite controller that synergistically combines a Super-Twisting Sliding Mode Controller (STSM) with a Finite-Time Sliding Mode Observer (FTSMO) to advance the control of PMSM drives. The proposed strategy leverages the FTSMO for rapid, finite-time disturbance estimation, enabling precise feedforward compensation that significantly enhances the system's dynamic response and suppresses overshoot, particularly under load variations and parameter uncertainties. Through extensive experimental and simulation-based validation, this work confirms that the STSM+FTSMO controller demonstrably outperforms conventional methods, exhibiting superior performance in start-up speed, disturbance rejection, and steady-state accuracy.

REFERENCES

[1] W. Xu, A. K. Junejo, Y. Liu, and M. R. Islam, "Improved Continuous Fast Terminal Sliding Mode Control With Extended State Observer for Speed Regulation of PMSM Drive System," *IEEE Transactions on Vehicular Technology*, vol. 68, no. 11, pp. 10 465–10 476, Nov. 2019. [Online]. Available: https://ieeexplore.ieee.org/document/8753613

[2] Y. Lu, J. Huang, Z. Jiang, T. Tang, H. Tang, and L. Shi, "PID Adaptive Feedback Motor System Based on Neural Network," *IEEE Access*, vol. 12, pp. 60 149–60 154, 2024. [Online]. Available: https://ieeexplore.ieee.org/document/10507815

[3] Y. Yu, S. Hao, S. Guo, Z. Tang, and S. Chen, "Motor Torque Distribution Strategy for Different Tillage Modes of Agricultural Electric Tractors," *Agriculture*, vol. 12, no. 9, p. 1373, Sep. 2022. [Online]. Available: https://www.mdpi.com/2077-0472/12/9/1373

[4] J. Wu, J. Zhang, B. Nie, Y. Liu, and X. He, "Adaptive Control of PMSM Servo System for Steering-by-Wire System With Disturbances Observation," *IEEE Transactions on Transportation Electrification*, vol. 8, no. 2, pp. 2015–2028, Jun. 2022. [Online]. Available: https://ieeexplore.ieee.org/abstract/document/9615239

[5] J. Cui, "Optimal control of maximum torque current ratio for synchronous reluctance motor based on virtual signal injection algorithm," *Archives of Electrical Engineering; 2024; vol. 73; No 2; 451-466*, 2024, publisher: Polish Academy of Sciences. [Online]. Available: https://journals.pan.pl/dlibra/publication/149926/edition/131505

[6] M. Preindl and S. Bolognani, "Model Predictive Direct Speed Control with Finite Control Set of PMSM Drive Systems," *IEEE Transactions on Power Electronics*, vol. 28, no. 2, pp. 1007–1015, Feb. 2013. [Online]. Available: https://ieeexplore.ieee.org/document/6216441

[7] Y. Zhou, H. Li, R. Liu, and J. Mao, "Continuous Voltage Vector Model-Free Predictive Current Control of Surface Mounted Permanent Magnet Synchronous Motor," *IEEE Transactions on Energy Conversion*,

10

vol. 34, no. 2, pp. 899–908, Jun. 2019. [Online]. Available: https://ieeexplore.ieee.org/document/8453015

[8] F. Wang, D. Ke, X. Yu, and D. Huang, "Enhanced Predictive Model Based Deadbeat Control for PMSM Drives Using Exponential Extended State Observer," *IEEE Transactions on Industrial Electronics*, vol. 69, no. 3, pp. 2357–2369, Mar. 2022. [Online]. Available: https://ieeexplore.ieee.org/document/9380958

[9] H.-Y. Tang, D.-Z. Xu, and Q. Sha, "Study on model predictive control of dual three-phase permanent magnet synchronous motor based on biplane virtual voltage vector," *Archives of Electrical Engineering; 2024; vol. 73; No 4; 869-890*, 2024, publisher: Polish Academy of Sciences. [Online]. Available: https://journals.pan.pl/dlibra/publication/152100/edition/133378

[10] S.-H. Chang, P.-Y. Chen, Y.-H. Ting, and S.-W. Hung, "Robust current control-based sliding mode control with simple uncertainties estimation in permanent magnet synchronous motor drive systems," *IET Electric Power Applications*, vol. 4, no. 6, pp. 441–450, Jul. 2010. [Online]. Available: http://digital-library.theiet.org/doi/10.1049/iet-epa.2009.0146

[11] Y. A.-R. I. Mohamed and E. F. El-Saadany, "A Current Control Scheme With an Adaptive Internal Model for Torque Ripple Minimization and Robust Current Regulation in PMSM Drive Systems," *IEEE Transactions on Energy Conversion*, vol. 23, no. 1, pp. 92–100, Mar. 2008. [Online]. Available: https://ieeexplore.ieee.org/document/4453985

[12] M. Nicola, C.-I. Nicola, and D. Seliteanu, "Improvement of PMSM Sensorless Control Based on Synergetic and Sliding Mode Controllers Using a Reinforcement Learning Deep Deterministic Policy Gradient Agent," *Energies*, vol. 15, no. 6, p. 2208, Mar. 2022. [Online]. Available: https://www.mdpi.com/1996-1073/15/6/2208

[13] S. Lixian and W. Rahiman, "A Compound Control for Hybrid Stepper Motor Based on PI and Sliding Mode Control," *IEEE Access*, vol. 12, pp. 163 536–163 550, 2024. [Online]. Available: https://ieeexplore.ieee.org/document/10741576

[14] X. Zhang, L. Sun, K. Zhao, and L. Sun, "Nonlinear Speed Control for PMSM System Using Sliding-Mode Control and Disturbance Compensation Techniques," *IEEE Transactions on Power Electronics*, vol. 28, no. 3, pp. 1358–1365, Mar. 2013. [Online]. Available: https://ieeexplore.ieee.org/document/6236202

[15] A. Wang, X. Jia, and S. Dong, "A New Exponential Reaching Law of Sliding Mode Control to Improve Performance of Permanent Magnet Synchronous Motor," *IEEE Transactions on Magnetics*, vol. 49, no. 5, pp. 2409–2412, May 2013. [Online]. Available: https://ieeexplore.ieee.org/abstract/document/6514698

[16] L. Qu, W. Qiao, and L. Qu, "An Extended-State-Observer-Based Sliding-Mode Speed Control for Permanent-Magnet Synchronous Motors," *IEEE Journal of Emerging and Selected Topics in Power Electronics*, vol. 9, no. 2, pp. 1605–1613, Apr. 2021. [Online]. Available: https://ieeexplore.ieee.org/document/9078744

[17] W. Liu, H. Ye, and X. Yang, "Super-Twisting Sliding Mode Control for the Trajectory Tracking of Underactuated USVs with Disturbances," *Journal of Marine Science and Engineering*, vol. 11, no. 3, p. 636, Mar. 2023, number: 3 Publisher: Multidisciplinary Digital Publishing Institute. [Online]. Available: https://www.mdpi.com/2077-1312/11/3/636

[18] Q. Hou, S. Ding, and X. Yu, "Composite Super-Twisting Sliding Mode Control Design for PMSM Speed Regulation Problem Based on a Novel Disturbance Observer," *IEEE Transactions on Energy Conversion*, vol. 36, no. 4, pp. 2591–2599, Dec. 2021. [Online]. Available: https://ieeexplore.ieee.org/abstract/document/9057471

[19] C. Dang, M. Dou, S. Yan, M. Dang, Y. Wang, D. Zhao, and Z. Hua, "An Improved Adaptive Sliding Mode Speed Control of PMSM Drives With an Extended State Observer," *IEEE Transactions on Energy Conversion*, vol. 39, no. 4, pp. 2349–2361, Dec. 2024. [Online]. Available: https://ieeexplore.ieee.org/abstract/document/10540230

[20] H. Lu, J. Li, S. Li, S. Wang, and Y. Xiao, "Finite-time extended state observer enhanced nonsingular terminal sliding mode control for buck converters in the presence of disturbances: design, analysis and experiments," *Nonlinear Dynamics*, vol. 112, no. 9, pp. 7113–7127, May 2024. [Online]. Available: https://doi.org/10.1007/s11071-024-09381-6

[21] Y. Wang, Y. Feng, X. Zhang, and J. Liang, "A New Reaching Law for Antidisturbance Sliding-Mode Control of PMSM Speed Regulation System," *IEEE Transactions on Power Electronics*, vol. 35, no. 4, pp. 4117–4126, Apr. 2020. [Online]. Available: https://ieeexplore.ieee.org/document/8789506

[22] Q. Hou and S. Ding, "Finite-Time Extended State Observer-Based Super-Twisting Sliding Mode Controller for PMSM Drives With Inertia Identification," *IEEE Transactions on Transportation Electrification*, vol. 8, no. 2, pp. 1918–1929, Jun. 2022. [Online]. Available: https://ieeexplore.ieee.org/document/9591643

[23] W. Xu, A. K. Junejo, Y. Tang, M. Shahab, H. U. Rahman Habib, Y. Liu, and S. Huang, "Composite Speed Control of PMSM Drive System Based on Finite Time Sliding Mode Observer," *IEEE Access*, vol. 9, pp. 151 803–151 813, 2021. [Online]. Available: https://ieeexplore.ieee.org/document/9600842

[24] A. LEVANT, "Sliding order and sliding accuracy in sliding mode control," *International Journal of Control*, Dec. 1993, publisher: Taylor & Francis Group. [Online]. Available: https://www.tandfonline.com/doi/abs/10.1080/00207179308923053

[25] J. A. Moreno and M. Osorio, "Strict Lyapunov Functions for the Super-Twisting Algorithm," *IEEE Transactions on Automatic Control*, vol. 57, no. 4, pp. 1035–1040, Apr. 2012. [Online]. Available: https://ieeexplore.ieee.org/document/6144710

[26] S. P. Bhat and D. S. Bernstein, "Finite-Time Stability of Continuous Autonomous Systems," *SIAM Journal on Control and Optimization*, Jul. 2006, publisher: Society for Industrial and Applied Mathematics. [Online]. Available: https://epubs.siam.org/doi/10.1137/S0363012997321358

[27] Y. Hong and Z.-P. Jiang, "Finite-Time Stabilization of Nonlinear Systems With Parametric and Dynamic Uncertainties," *IEEE Transactions on Automatic Control*, vol. 51, no. 12, pp. 1950–1956, Dec. 2006. [Online]. Available: http://ieeexplore.ieee.org/document/4026648/

[28] A. Levant, "Robust exact differentiation via sliding mode technique*," *Automatica*, vol. 34, no. 3, pp. 379–384, Mar. 1998. [Online]. Available: https://www.sciencedirect.com/science/article/pii/S0005109897002094

[29] A. Polyakov, "Nonlinear Feedback Design for Fixed-Time Stabilization of Linear Control Systems," *IEEE Transactions on Automatic Control*, vol. 57, no. 8, pp. 2106–2110, Aug. 2012. [Online]. Available: https://ieeexplore.ieee.org/document/6104367

[30] H. K. Khalil, *Nonlinear Systems*. Prentice Hall, 2002, google-Books-ID: t_d1QgAACAAJ.
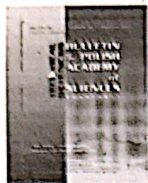
LICENSE TO PUBLISH

The following License to Publish ("License") must be signed and returned to the Journal Owner before a manuscript can be published. If the copyright in the contribution is owned by the author's employer, the employer or an authorized representative must sign this form. In the event that the Journal Owner decides not to publish the Work, this License shall be null and void.

Please read the terms of this agreement, print initial page 1, print and sign page 2, scan and upload the document as one file according to the Editors' guidelines (submit via Editorial System).

Article entitled ("Work" or "Article"):
High-Performance Control of Permanent Magnet Synchronous Motor using a Finite-Time Sliding Mode Observer and Super-Twisting Algorithm
Author/s: (also referred to as "Licensor/s")

Jing Nie ,Yong Li,Gang Li

Corresponding author: (if more than one author)

Yong Li

Journal Name
Bulletin of the Polish Academy of Sciences Technical Sciences

Journal Owner
Polish Academy of Sciences

1. License

The use of the article will be governed by the Creative Commons Attribution license CC BY 4.0 as currently displayed on https://creativecommons.org/licenses/by/4.0/.

2. Author's Warranties

The author warrants that the article is original, written by stated author/s, has not been published before, contains no unlawful statements, does not infringe the rights of others, is subject to copyright that is vested exclusively in the author and free of any third party rights, and that any necessary written permissions to quote from other sources have been obtained by the author/s. The undersigned also warrants that the manuscript (or its essential substance) has not been published other than as an abstract or doctoral thesis and has not been submitted for consideration elsewhere, for print, electronic or digital publication.

3. User Rights

Under the Creative Commons Attribution license, the author(s) and users are free to share (copy, distribute and transmit the contribution) under the following conditions:
1. They must attribute the contribution in the manner specified by the author or licensor,
2. They may use this contribution for commercial purposes,
3. They may alter, transform, or build upon this work.

4. Rights of Authors

Authors retain the following rights:
– copyright, and other proprietary rights relating to the article, such as patent rights,
– the right to use the substance of the article in future own works, including lectures and books,
– the right to reproduce the article for own purposes, provided the copies are not offered for sale,
– the right to self-archive the article,
– the right to supervision over the integrity of the content of the work and its fair use.

1

5. Co-Authorship

If the article was prepared jointly with other authors, the signatory of this form warrants that he/she has been authorized by all co-authors to sign this agreement on their behalf, and agrees to inform his/her co-authors of the terms of this agreement.

6. Termination

This agreement can be terminated by the author or the Journal Owner upon two months' notice where the other party has materially breached this agreement and failed to remedy such breach within a month of being given the terminating party's notice requesting such breach to be remedied. No breach or violation of this agreement will cause this agreement or any license granted in it to terminate automatically or affect the definition of the Journal Owner. The author and the Journal Owner may agree to terminate this agreement at any time. This agreement or any license granted in it cannot be terminated otherwise than in accordance with this section 6. This License shall remain in effect throughout the term of copyright in the Work and may not be revoked without the express written consent of both parties.
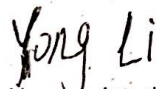
7. Royalties

This agreement entitles the author to no royalties or other fees. To such extent as legally permissible, the author waives his or her right to collect royalties relative to the article in respect of any use of the article by the Journal Owner or its sublicensee.

8. Miscellaneous

The Journal Owner will publish the article (or have it published) in the Journal if the article's editorial process is successfully completed and the Journal Owner or its sublicensee has become obligated to have the article published. Where such obligation depends on the payment of a fee, it shall not be deemed to exist until such time as that fee is paid. The Journal Owner may conform the article to a style of punctuation, spelling, capitalization and usage that it deems appropriate. The author acknowledges that the article may be published so that it will be publicly accessible, and such access will be free of charge for the readers. The Journal Owner will be allowed to sublicense the rights that are licensed to it under this agreement. This agreement will be governed by the laws of Poland.

By signing this License, Author(s) warrant(s) that they have the full power to enter into this agreement. This License shall remain in effect throughout the term of copyright in the Work and may not be revoked without the express written consent of both parties.

Author's (Corresponding Author's) Signature (to be signed only by the corresponding Author):

Yong Li

Name printed:

Yong Li

Date:

25/09/2025